Negative magnetopolarization in thermally annealed self-assembled quantum dots

E. Margapoti,[1,2] L. Worschech,[1,2] S. Mahapatra,[1,3] K. Brunner,[1,3] A. Forchel,[1,2] Fabrizio M. Alves,[4] V. Lopez-Richard,[4] G. E. Marques,[4] and C. Bougerol[5]

[1]*Physikalisches Institut, Universität Würzburg, Am Hubland, 97074 Würzburg, Germany*

[2]*Technische Physik, Universität Würzburg, Am Hubland, 97074 Würzburg, Germany*

[3]*Experimentelle Physik III, Universität Würzburg, Am Hubland, 97074 Würzburg, Germany*

[4]*Departamento de Física, Universidade Federal de São Carlos, 13560-905 São Carlos, São Paulo, Brazil*

[5]*CEA-CNRS NPSC, SP2M/DRFMC/CEA-Grenoble, 17 rue des Martyrs, 38054 Grenoble Cedex, France*

(Received 16 April 2007; revised manuscript received 17 October 2007; published 21 February 2008)

A negative magnetic dispersion of the degree of circular polarization is reported for the photoluminescence of self-assembled ZnCdSe quantum dots (QDs) after a postgrowth thermal annealing (TA) treatment. Multiband calculations in the framework of the $\mathbf{k}\cdot\mathbf{p}$ model reveal that the phenomenon is explicable considering, apart from the changes in the confinement and composition of the QDs due to TA-induced Zn-Cd interdiffusion, the presence of extra charges of one kind within the structure.

DOI: 10.1103/PhysRevB.77.073308 PACS number(s): 78.55.Et, 78.20.Bh, 78.20.Ls, 78.67.Hc

Magneto-optical properties of self-assembled semiconductor quantum dots (QDs) have emerged in the recent years as a widely pursued field of research,[1,2] triggered by the possibility of using the spin degree of freedom of a three-dimensionally confined exciton to realize the basic building blocks of quantum information processing.[3,4] The magneto-optical response of an individual QD and an ensemble of QDs yields much fundamental information, imperative to achieving this goal, i.e., the spin splitting of the exciton ground state[5–10] and the spin lifetime of the electron and the hole comprising the exciton.[11,12] The polarization behavior of photoluminescence (PL), emitting from QDs in the presence of a magnetic field, serves as an excellent tool to probe the exciton spin dynamics in QDs.

In this work, the evolution of the degree of circular polarization (DCP) has been studied for the magneto-PL of epitaxially self-assembled ZnCdSe QDs before and after a postgrowth rapid thermal annealing (TA) treatment. While for the as-grown (not-annealed) QDs the DCP undergoes a reversal from positive to negative sign beyond a magnetic field strength of $B=3$ T, we demonstrate here that the DCP corresponding to the annealed QDs exhibits a negative magnetic dispersion in the entire range of $B=0-5$ T. A multiband calculation in the framework of the $\mathbf{k}\cdot\mathbf{p}$ theory reveals that apart from changes in the composition and configuration of the QDs due to TA-induced interdiffusion of Zn and Cd, the presence of extra charges of one kind needs to be taken into account. Albeit spin splitting and DCP of magneto-PL have been studied for quantum wells of a few systems,[10,13] such studies for three-dimensionally confined excitons, especially their evolution with changing composition and confinement of QDs, to the best of our knowledge, has not been pursued so far.

The samples under investigation were grown by molecular beam epitaxy on top of homoepitaxially grown undoped GaAs buffers on GaAs:Si (100) substrates. The CdSe QD layer was embedded between a 50 nm thick ZnSe buffer layer, grown atop a GaAs pseudosubstrate, and a 25 nm thick ZnSe cap layer. In this manner, two different samples were realized with the CdSe layer either nominally 2 or 1 ML thick. In CdSe/ZnSe heteroepitaxy, QDs ensue due to fluctuations in Cd concentration in an alloyed $Zn_{1-x}Cd_xSe$ quantum-well (QW)-like structure.

Postgrowth rapid thermal annealing of the samples was performed in a N_2 environment at $T_A=500$ °C. Thermal annealing induces a pronounced blueshift of the PL spectra as demonstrated for 2 ML QDs in Fig. 1. Prior to TA, the QD spectrum is broad with a typical full width at half maximum of about 35 meV attributed to QD inhomogeneities. The peak maximum has an energy of 2.42 eV for the as-grown QDs. As shown in Fig. 1, blueshifts of the PL peak up to 170 meV were observed for QDs annealed for $t_A=50$ s. Evidently, the full width at half maximum is decreased in annealed QDs compared to as-grown QDs.

Spectral narrowing by TA is well known and was also observed for QDs realized in other material systems, e.g., by Kobayashi and Yamaguchi,[14] and associated with a TA enhancement of the QD homogeneity. From a close inspection of Fig. 1, one can identify asymmetries in the PL spectrum. For example, for the as-grown QDs at the low-energy site, a second peak with much lower intensity and an energy of 2.37 eV can be found by fitting the corresponding spectrum. Also, the spectrum of the annealed QDs ($t_A=50$ s) has, e.g., at the high-energy site, a shoulder. However, from the absence of thermalization between these components, we conclude that the distribution of QDs is at least bimodal. Bimodal distributions of QDs were observed by different groups, e.g., by Lee *et al.*[15] in the case of InAs QDs, and attributed to the presence of small and large dots.

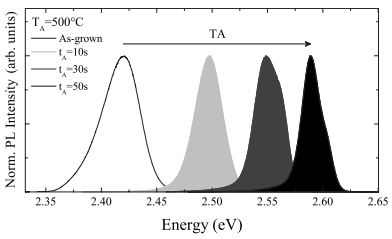

FIG. 1. Photoluminescence spectra of 2 ML QDs conducted prior to TA and after different TA procedures performed at a temperature of $T_A=500$ °C but different TA durations $t_A=10$, 30, and 50 s. Due to TA, the peak maximum shifts to higher energies accompanied by a narrowing of the QD spectrum.

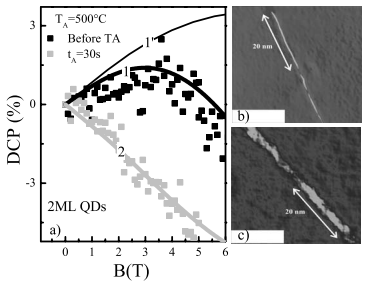

FIG. 2. Squares represent the DCP of 2 ML $Zn_{1-x}Cd_xSe$ QD luminescence recorded at the peak maximum. Solid curves are the corresponding theoretical values with $R=100$ Å: (1) $x=0.45$, $L_z=34.2$ Å, $n_h=1.67n_{dot}$; (1′) $x=0.45$, $L_z=34.2$ Å, $n_h=n_e=1.8n_{dot}$; (2) $x=0.16$, $L_z=82$ Å, $n_h=1.82n_{dot}$; (b) HRTEM pictures taken prior to and (c) after thermal annealing for 30 s at $T_A=500$ °C.

To probe the annealing-induced evolution of the magneto-optical properties of the QD ensembles, magnetophotoluminescence measurements were carried out in a liquid He bath cryostat at a temperature of 2 K. Magnetic fields were applied parallel to the growth direction (Faraday geometry). The PL was excited with the 405 nm line of a solid state continuous wave laser. In order to investigate the circular polarization of the QD luminescence, a 50 kHz photoelastic modulator operating as a $\lambda/4$ plate in combination with a linear polarizer was placed in front of the monochromator. For the magnetic field dependent polarization measurements, we detected the degree of circular polarization $\mathrm{DCP}=(I^- - I^+)/(I^- + I^+)$, where I^+ (I^-) represents the intensity of σ^+ (σ^-) polarized QD emission, recorded at the peak maximum. These measurements were performed for the two samples prior to and after TA.

The DCP for the 2 ML QD luminescence versus the magnetic field strength is shown in the left part of Fig. 2(a) for a 2 ML QD sample prior to and after TA at a temperature $T_A=500$ °C and for $t_A=30$ s. A positive DCP is observed for these QDs prior to TA up to $B=5$ T. Interestingly, above this critical magnetic field, the DCP is negative, which indicates a magnetic field induced mixing of the excitonic states.[10] Such a finding reflects an anomalous Zeeman effect. In contrast, after TA, the QDs show a negative DCP for all values of magnetic field strength. Figure 3 shows the dependence of the DCP on B for the 1 ML QDs before and after TA at $T_A=500$ °C and for $t_A=20$ and 30 s. Evidently, the QD luminescence prior to annealing exhibits a positive DCP, which increases monotonically until 5 T. After annealing for 20 s, the DCP is close to zero and for $t_A=30$ s, it shows a negative dispersion. Thus, only for the 2 ML QDs prior to TA is a magnetic field induced sign reversal of the DCP observed. PL from both 1 ML QDs and the 2 ML QDs exhibits a negative DCP after annealing for $t_A=30$ s.

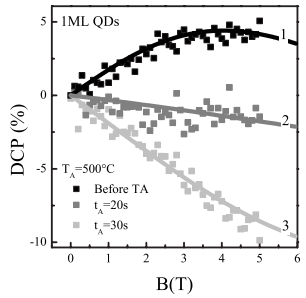

FIG. 3. Squares represent the experimental data for the gradual variation in the DCP of 1 ML QD luminescence for different annealing times. Solid curves are the corresponding theoretical values with $R=100$ Å: (1) $x=0.45$, $L_z=17$ Å, $n_h=1.33n_{dot}$; (2) $x=0.2$, $L_z=32$ Å, $n_h=1.85n_{dot}$; (3) $x=0.16$, $L_z=40$ Å, $n_h=1.75n_{dot}$.

We ascribe this behavior to TA-induced changes of the QD confinement and Cd-Zn content. Such assumptions are justified by high resolution transmission electron microscope (HRTEM) images recorded for the structure prior to TA and also, for comparison, after TA. The cross-sectional HRTEM images were obtained with a Jeol 4000EX microscope, operated at 400 kV. A Wiener filter was first applied to the images to remove the noise.[16] Then, the images were analyzed by the geometrical phase method,[17,18] which allowed us to get the lattice parameter along the growth direction, z, taking the lower ZnSe barrier as a reference. In Figs. 2(b) and 2(c), cross-section images of the variations of the lattice parameter are shown. Bright contrasts represent regions with Cd content. As indicated by the white arrow, a typical diameter determined for QDs prior to TA is about 20 nm. Also, the variation of the lattice parameter along the growth direction (z direction) was obtained from high resolution off axis images taken after tilting the sample by 10° around the z axis from the [110] zone axis (not shown). Hereby, we determined a QD extension along the direction of growth, $L_z=2$ nm. A similar analysis was made with the thermally annealed sample, too. We emphasize that the sample was annealed first and then prepared for cross-sectional electron microscopy. Here, the QDs have an extension of 6–8 nm in the growth direction. Typical diameters in the range of 20 nm were determined [Fig. 2(c)].

For the theoretical description, we have considered the QDs embedded in a QW-like structure. The spatial confinement of holes and electrons in the theoretical simulation is defined by an in-plane potential, $V_{x,y}=1/2m_{x,y}\omega_0^2(x^2+y^2)$, where $m_{x,y}$ is the carrier in-plane effective mass and $\omega_0^2=\hbar/(m_0R^2)$ is the parabolic confinement strength in terms of the effective lateral extension of the QD, R.[19] For the longitudinal direction, we assume a hard wall QW with height L_z. The unperturbed Hamiltonian has the well-known Fock-Darwin solution.[19] The kinetic energy for the valence (conduction) band is treated by the 4×4 (2×2) Luttinger coupled (parabolic uncoupled) Hamiltonian.

This multiband calculation shows how the spin splitting of the ground states of the electrons and heavy hole depends on the QD parameters. The Cd-content dependence has been introduced from the reported values of the band parameters of $Zn_{1-x}Cd_xSe$.[20,21] Due to lack of reported parameters, a linear interpolation between the corresponding values of ZnSe and CdSe has been assumed for the alloy composition. In Figs. 4(a) and 4(b), the corresponding Zeeman splittings for the first conduction and the topmost valence band levels are shown for various Cd-content values. Although the conduction band is slightly affected by the alloy composition, it is the valence band that responds in a much stronger way. The Zeeman splitting of the valence band ground state changes slope with the magnetic field and its sign beyond a

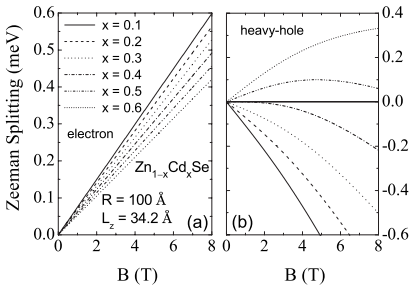

FIG. 4. Calculated Zeeman splitting for the (a) conduction and (b) valence ground states of the QD as a function of the magnetic field and for different Cd contents x.

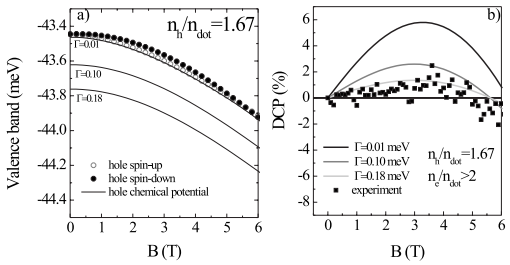

FIG. 5. (a) Calculated chemical potential in the valence band for various values of Γ for a fixed $n_{hh}/n_{dot}=1.67$. (b) Calculated DCP for the quasi-Fermi levels shown in (a). The experimental values are shown with square symbols.

certain Cd concentration. This is caused by the coupling between the light- and the heavy-hole states. Such an effect leads to an inversion in the occupation of the spin-split hole levels which, in turn, results in a sign reversal of the DCP, in good agreement with the trends shown in Figs. 2(a)–2(c).

The interplay of alloy composition and QD size will finally affect the effective Zeeman splitting of the states involved in the optical transition. However, the spin splitting is not the only feature that affects the DCP. DCP combines the effect of the spin polarization of both holes and electrons; thus, an analysis must be developed considering the carrier occupation in both conduction and valence band ground states.

In order to obtain the DCP of the PL emissions, we must first obtain the electrochemical potential for electrons and holes independently. We have assumed that for a given QD density per unit volume, n_{dot}, the density of states for the ground state spin-split levels in both conduction and valence bands can be calculated as

$$D_{e(hh)}(E) = \frac{n_{dot}}{\pi} \sum_{j,\sigma=\pm} \frac{\Gamma}{[E - E^{j,\sigma}_{e(hh)}(B)]^2 + \Gamma^2}, \tag{1}$$

with $E^{j,+}_{e(hh)}$ and $E^{j,-}_{e(hh)}$ being the spin-split energies for electrons (holes) in the state j, calculated from the multiband model, and Γ is an energy dispersion. Its nature will be explained later. The three-dimensional (3D) carrier density would then be

$$n_{e(hh)} = \int f_{e(hh)}(E) D_{e(hh)}(E) dE, \tag{2}$$

where $f_{e(hh)}(E) = \left\{1 + \exp\left(\frac{E-\mu_{e(hh)}}{KT}\right)\right\}^{-1}$ is the Fermi distribution function. The value of the chemical potential for electrons (holes), $\mu_{e(hh)}$, is obtained from Eqs. (2) and (1), given the 3D density of carriers, $n_{e(hh)}$, in terms of the QD density n_{dot}.

The intensity maximum of the optical recombination with circular polarization ($\sigma^{\pm}$) is taken to be proportional to

$$I^{\pm} \propto |P^{\pm}|^2 f_e(E^{1,\pm}_e) f_{hh}(E^{1,\pm}_{hh}), \tag{3}$$

where $E^{1,+}_{e(hh)}$ and $E^{1,-}_{e(hh)}$ are the energies of the spin-split ground states of electrons and holes, calculated from the multiband model. $|P^{\pm}|^2$ are the values of the oscillator strengths for each spin-polarized transition in the dipole approximation. These functions depend on the values of the external fields applied to the sample, its composition, and confinement geometry.

An important assumption is to consider an excess density of electrons compared to that of the holes. It is well known that II selenides exhibit an unintentional n-type conductivity, often attributed to native defects.[22] Electrons from certain donor-type native defects,[23] as well as from the n-type GaAs substrate, might relax into the QDs both during epitaxial growth and postgrowth TA, rendering the QDs negatively charged. Thus, we have assumed $n_e/n_h > 1$ to account for the charge imbalance and also that $n_e \geq 2n_{dot}$ (under this condition, the spin occupation for electron ground states will be the same for both spin-up and spin-down levels).

In order to explain the physical meaning of the Γ parameter introduced in Eq. (1), the electrochemical potential in the valence band is shown in Fig. 5(a) for various values of Γ at a fixed value of $n_{hh}/n_{dot}=1.67$. The corresponding degree of circular polarization for the selected Fermi energy vs B is shown in Fig. 5(b). The nature of the parameter Γ accounts for scattering processes that might induce a level broadening, such as spin relaxation. In order to fit the experimental value of the DCP, we just need a position of the quasi-Fermi level. Thus, the value of Γ will only depend on the relation n_{hh}/n_{dot} that we introduce.

Therefore, our model provides information on the electrochemical potential of electrons and holes as well as the broadening of QD states due to scattering. We emphasize that other information can be extracted, e.g., a ratio of the spin relaxation time τ_S with the electron-hole recombination time τ_R, by comparing our model with the model of Mackowski *et al.*[9] In the model of Mackowski *et al.*, the case of an optical generation of spin-polarized carriers was considered. Since the experiments were done by using a linear polarized source in the present work, which implies equal spin generation rates, according to Mackowski *et al.*,[9] we can rewrite the equation for degree of circular polarization as

$$\mathrm{DCP} = \tau_R(1 - e^{\Delta E/KT})/[\tau_R + e^{\Delta E/KT}(\tau_R + \tau_S)], \tag{4}$$

where ΔE is the Zeeman splitting of the CdSe QDs. Setting the ratio of the spin and exciton relaxation times $\tau = \tau_S/\tau_R = 10$, as reported in Ref. 9, it is possible to fit the experimental data and also to reproduce our theoretical data if we take into account the above discussed charge imbalance (see Fig. 6). As a result from our model, the same information ex-

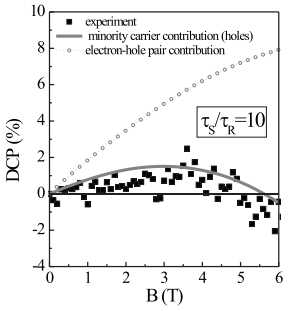

FIG. 6. Calculated DCP using Eq. (4) with ΔE given by the energy splitting of electron-hole pairs (dashed) or just hole levels (solid curve). The experimental values are shown with square symbols.

tracted from the model of Mackowski *et al.* can be determined. In addition, one can also describe the electrochemical potential of electrons and holes. We should point out that Eq. (4) needs to be modified when the change in sign of the DCP is considered. Precisely, in order to fit the experimental data, from 3.5 to 6 T, the sign of the right side of Eq. (4) and ΔE is changed.

In order to calculate the DCP shown in Figs. 2 and 3, we have assumed a broadening $\Gamma=0.18$ meV for a nominal temperature $T=2$ K.

In Fig. 2(a), the curve labeled 1 represents the result obtained by fixing $x=0.45$, $L_z=34.2$ Å, $R=100$ Å with $n_h=1.67n_{dot}$. Given the electron excess, the DCP sign reversal is totally ascribed to the valence band Zeeman splitting inversion for the given parameters. The hole density decrease from 1 to 1′ leads to an increase of the DCP in absolute values. Curve 2 corresponds to $x=0.16$, $L_z=82$ Å, $R=100$ Å with $n_h=1.82n_{dot}$. We emphasize that these values have been also fitted to describe the peak position of the QD luminescence, in excellent agreement with the experimental observation. The experimentally predicted Cd-content decrease and QD-height increase have been theoretically confirmed as demonstrated by the different sets of QD parameters used to obtain curves 1 ($x=0.45$, $L_z=34.2$ Å) and 2 ($x=0.16$, $L_z=82$ Å). The DCP tends toward negative values as the QD height increases and the density of carriers imbalance decreases.

The case of the 1 ML QD sample, shown in Fig. 3, also confirms these tendencies. In this case, the initial values of the QD parameters, which fit better to the experimental data before TA, correspond to $x=0.45$, $L_z=17$ Å, $R=100$ Å. Note that $L_z=17$ Å for this case is exactly half the value of $L_z=34.2$ Å used to fit the result for the 2 ML QD sample, as expected. This result is an unambiguous indication of the parameter trends during the process of QD assembling prior to TA. The change in the QD parameters with time during annealing can be followed by curves 1–3 in Fig. 3, where the Cd content and height of the QDs have been varied as (1) $x=0.45$, $L_z=17$ Å, (2) $x=0.2$, $L_z=32$ Å, and (3) $x=0.16$, $L_z=40$ Å.

We may thus assert that the process of thermal annealing is accompanied by two dynamic effects: decrease of the Cd content and the tendency toward an increase of the QD height, both observed experimentally [see Fig. 2(c)]. Given that the minimum area is attained at $\lim_{t_A\to\infty}\frac{L_z}{R}=1$ for a constant volume in a cylindrical system, a tendency to minimize the external area could be a plausible explanation for the QD-size change during the TA process.

In summary, we have been able to describe the dynamics of size and composition change of $Zn_{1-x}Cd_xSe$ quantum dots during postgrowth rapid thermal annealing and its effects on the distribution of spin-polarized electrons and holes in semiconductor QDs. A tendency toward a configuration with a minimum area has been indicated along with changes in the alloy composition both by experimental observation and a multiband theoretical calculation. The effects of TA-induced changes in the configuration and composition of the QDs on the valence band levels predominate over those on the conduction states. The anomalous DCP response of the QDs in magnetic fields can be unambiguously related to the effective spin occupation of holes in an *n*-type sample and the complex valence band dispersion with field due to heavy- and light-hole coupling.

F.M.A., V.L.-R., and G.E.M. acknowledge financial support from Brazilian agencies FAPESP and CNPq. This work was financially supported in part by the DFG through SFB 410 and by the state of Bavaria.

[1] R. Rinaldi *et al.*, Phys. Rev. Lett. **77**, 342 (1996).
[2] M. Bayer *et al.*, Phys. Rev. Lett. **82**, 1748 (1999).
[3] W. H. Jiang *et al.*, J. Vac. Sci. Technol. A **24**, 700 (2006).
[4] A. Van der Ven and G. Ceder, Phys. Rev. Lett. **94**, 045901 (2005).
[5] R. Hanson *et al.*, Phys. Rev. Lett. **97**, 087601 (2006).
[6] S. Laurent *et al.*, Phys. Rev. B **73**, 235302 (2006).
[7] F. Takanoa *et al.*, Physica E (Amsterdam) **34**, 389 (2006).
[8] R. Danneau *et al.*, Phys. Rev. Lett. **97**, 026403 (2006).
[9] S. Mackowski *et al.*, Appl. Phys. Lett. **83**, 5524 (2003).
[10] N. J. Traynor, R. T. Harley, and R. J. Warburton, Phys. Rev. B **51**, 7361 (1995).
[11] S. Kono *et al.*, Phys. Rev. B **72**, 155307 (2005).
[12] M. Califano, G. Bester, and A. Zunger, Nano Lett. **3**, 1197 (2003).
[13] R. Kotlyar *et al.*, Phys. Rev. B **63**, 085310 (2001).
[14] Y. Kobayashi and K. Yamaguchi, Appl. Surf. Sci. **244**, 88 (2005).
[15] S. J. Lee *et al.*, J. Korean Phys. Soc. **42**, 686 (2003).
[16] P. L. Galindo, Strain determination software, Universidad Cadiz, Spain.
[17] M. J. Hytch, E. Snoeck, and R. Kilaas, Ultramicroscopy **74**, 131 (1998).
[18] W. Neumann *et al.*, J. Microsc. **223**, 200 (2006).
[19] C. F. Destefani, S. E. Ulloa, and G. E. Marques, Phys. Rev. B **69**, 125302 (2004).
[20] *Landölt-Börnstein Comprehensive Index*, edited by O. Madelung and W. Martienssen (Springer, Berlin, 1996).
[21] S. Z. Karazhanov and L. Yan Voon, Semiconductors **39**, 161 (2005).
[22] C. G. Van de Walle, Phys. Status Solidi B **229**, 221 (2002).
[23] T. Yao, J. Cryst. Growth **72**, 31 (1985).